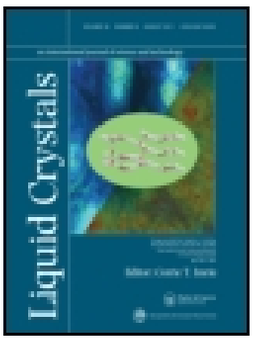

Liquid Crystals

ISSN: 0267-8292 (Print) 1366-5855 (Online) Journal homepage: http://www.tandfonline.com/loi/tlct20

Evaluation of phase state and rotational viscosity of fast response liquid crystals using a fully atomistic molecular dynamics

Qidong Wang, Guiyang Zhang, Yonggang Liu, Lishuang Yao, Dayu Li, Shaoxin Wang, Zhaoliang Cao, Quanquan Mu, Chengliang Yang, Li Xuan, Xinghai Lu & Zenghui Peng

To cite this article: Qidong Wang, Guiyang Zhang, Yonggang Liu, Lishuang Yao, Dayu Li, Shaoxin Wang, Zhaoliang Cao, Quanquan Mu, Chengliang Yang, Li Xuan, Xinghai Lu & Zenghui Peng (2017): Evaluation of phase state and rotational viscosity of fast response liquid crystals using a fully atomistic molecular dynamics, Liquid Crystals, DOI: 10.1080/02678292.2017.1302009

To link to this article: http://dx.doi.org/10.1080/02678292.2017.1302009

Published online: 15 Mar 2017.

LIQUID CRYSTALS, 2017
http://dx.doi.org/10.1080/02678292.2017.1302009

Taylor & Francis
Taylor & Francis Group

ARTICLE

Evaluation of phase state and rotational viscosity of fast response liquid crystals using a fully atomistic molecular dynamics

Qidong Wang[a], Guiyang Zhang[b], Yonggang Liu[a], Lishuang Yao[a], Dayu Li[a], Shaoxin Wang[a], Zhaoliang Cao[a], Quanquan Mu[a], Chengliang Yang[a], Li Xuan[a], Xinghai Lu[a] and Zenghui Peng[a]

[a]State Key Laboratory of Applied Optics, Changchun Institute of Optics, Fine Mechanics and Physics, Chinese Academy of Sciences, Changchun, Jilin, China; [b]University of Chinese Academy of Sciences, Beijing, China

ABSTRACT

Rational design of liquid crystals (LCs) with excellent phase state and rotational viscosity has been a crucial technique for response speed improvement of LC wavefront corrector. A complete process for theoretically evaluating the phase state and rotational viscosity of fast response LCs using a fully atomistic molecular dynamics is reported. Predicted trends in molecular order, phase-transition temperature between metastable states and rotational viscosity show excellent agreement with experimental results. We also demonstrate that overestimation of the attraction both between and within molecules in the general Amber force field mainly leads to a systematic shift in the phase-transition temperature, rotational viscosity and figure-of-merit for fast response LCs. With further optimisations of intermolecular potential, simulation procedure and data processing, this fully atomistic simulation will be a useful evaluation method of response performance of LC materials.

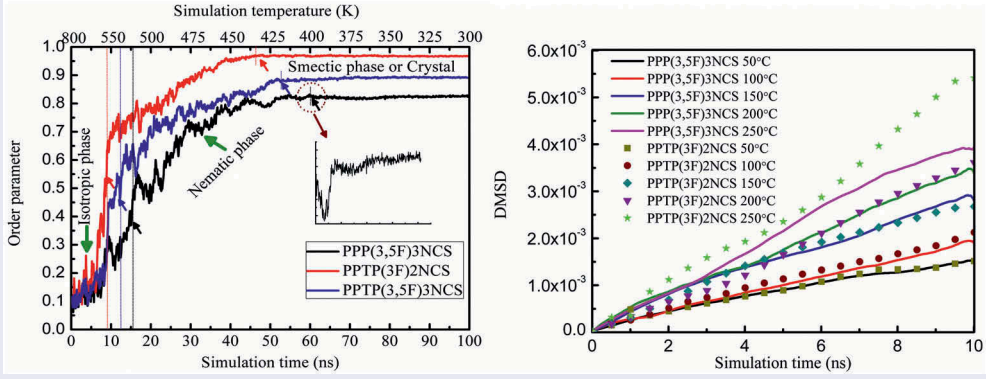

ARTICLE HISTORY
Received 12 November 2016
Accepted 28 February 2017

KEYWORDS
Molecular dynamics; liquid crystal; phase state; rotational viscosity; response performance

1. Introduction

In recent years, with the breakthrough of some key technologies, liquid crystal (LC) adaptive optics systems (LCAOSs) have been widely used in many scientific and medical applications, especially in the large-aperture telescopes, to improve the image quality [1,2]. In LCAOSs, LC wavefront corrector (LCWFC) is a critical component, which is used to real-timely compensate the optical aberration in the system [3]. For a long time, a slow response speed, typically about 10 ms, has been a main limiting factor for widely application of LCAOSs. For the telescopes with apertures of tens or even hundreds of metres, sub-millisecond response speed is needed. Despite many efforts, such as overvoltage drive technology [4], transient nematic effect [5] and optimal cell gap effect [6], have been recently made to improve the response speed of LCWFC, the essential way to figure out this situation is the response performance improvement of LC materials. Dual frequency [7], ferroelectric [8] and polymer network LC materials [9] show a captivating response performance with a sub-millisecond response time; however, due to high-voltage requirement and complexity of control method, the dual frequency and polymer network LCWFCs are improper to be applied to large-aperture telescopes. The bistability and low grayscale of ferroelectric LCs limit their effectiveness in LCWFCs [10]. Compared with the LC materials mentioned above, high-performance nematic LCs should be relatively ideal with a suitable driving voltage and a reliable preparation technique.

CONTACT Zenghui Peng peng@ciomp.ac.cn.

Based on the elastic theory of LC, response speed of nematic LCWFCs is proportional to the square of birefringence Δn at a specific modulation quantity ($\tau_{\text{off}} = \gamma_1\lambda^2/\pi^2\Delta n^2 K_{11}$). The most effective way to increase birefringence Δn is to elongate the π-electron conjugation lengths of LC monomers [11,12]. However, high phase-transition temperature and increased viscosity always come into being along with this extending of π-electron conjugation length. The LC compound with a high phase-transition temperature goes against mixing of LC material and it is difficult or even impossible to be applied. Obviously, according to the above formula, the increased rotational viscosity exerts an unfavourable influence on the response speed of nematic LCWFCs. Thus, in order to rationally design a fast response LC compound, a complete evaluation or quantitative analysis of birefringence, phase state and rotational viscosity is necessary.

The birefringence Δn of nematic LCs can be obtained by the Vuks equation [13]. A lot of research reveal that there are significant relationships between the calculated and measured data with correlation coefficients between 0.85 and 0.95, that is, the Vuks model behaves well to predict the birefringence Δn of nematic LCs. From microcosmic or molecular aspects, the birefringence Δn of nematic LCs can be regarded as a 'static character'; however, phase state and viscosity belong to the dynamic characteristics which involve a molecular movement or reorientation; so both of them need to be studied by a LC molecular dynamics (MD). Compared with hard nonspherical models (e.g. hard spherocylinders) or soft nonspherical models (e.g. Gay–Berne potential), a fully atomistic MD can provide a clearer and deeper description of the intra- and intermolecular interactions between LC molecules [14–16]. Recently, some noteworthy achievements have been made using all-atom models to investigate the phase state and viscosity of LCs with a huge increase of computer power. An example of this was provided by the work of Pelaez and Wilson [15], who achieved the growth of a nematic phase of E7 directly from an isotropic liquid over a 100 ns period for an all-atom model and also studied orientational and dipole order within the nematic phase. Then, Chami et al. were able to give the instantaneous LC order parameter of 8CB at different simulation temperatures for 150 molecules and achieved thermodynamically stable states across the N–I region of 8CB [17]. In general, there are two methods to calculate the rotational viscosity of LCs: equilibrium and non-equilibrium MD methods. Although the non-equilibrium MD method was used by Kuwajima et al. to obtain a satisfactory calculated value of viscosity in which the director of nematic systems is forced to rotate by an artificial force termed aligning force [18], this method is not particularly attractive for a fully atomistic MD, as the director must be constrained or reorientated and these tasks are not simple at an atomistic level [14]. Instead, equilibrium MD method is more accessible. Researchers such as Zakharov and Cheung [19–24] had calculated rotational viscosities of some LCs using this equilibrium MD method.

Focusing on the actual application, in this paper, we provide a complete method for evaluating the phase state and rotational viscosity of fast response LCs based on a fully atomistic MD. The prediction of phase-transition temperatures between metastable states and rotational viscosities of such LCs will become the emphases attention problems. This paper is organised as follows: first, we describe the MD models and simulation details; the computational method of rotational viscosity will also be presented. This is followed by a detailed description of simulation of fast response LCs, including the characteristics of phase state and rotational viscosity. What's more, to characterise the performance of fast response LCs, a figure-of-merit (FoM) [25] which takes phase change and response time into account has been discussed. Finally, a summary of results and outlook for further studies are provided.

2. Simulation model and methodology

2.1. Force field parameters

Force field is the cornerstone of MD simulation. A successful force field in LC molecular design should have the traits of universality and practicability. The general Amber force field (GAFF) [26–28] is designed to be compatible with existing Amber force fields and contains parameters for most organic and pharmaceutical molecules [26]. A simple functional form is used to describe the structures and nonbonded energies:

$$V = \sum_{\text{bond}} \frac{1}{2}K_l(l-l_0)^2 + \sum_{\text{angle}} \frac{1}{2}K_\theta(\theta-\theta_0)^2 + \sum_{\text{dihedrals}} \frac{V_n}{2}[1+\cos(n\phi-\gamma)] + \sum_{i,j} \frac{1}{4\pi\varepsilon\varepsilon_o}\frac{q_i q_j}{r_{ij}} + \sum_{i,j} 4\varepsilon_{ij}\left(\left(\frac{\sigma_{ij}}{r_{ij}}\right)^{12} - \left(\frac{\sigma_{ij}}{r_{ij}}\right)^{6}\right) \quad (1)$$

Here, l, θ and $\varnothing$ are structural parameters and l_0, θ_0 are the equilibration ones, K_l, K_θ and V_n represent force constants, n is multiplicity and γ is the phase angle. The σ_{ij} and q characterise the nonbonded energies. The partial charges q are assigned using a restrained electrostatic potential [29] fit model which has a clear physical picture and a straightforward implementation scheme [26].

2.2. Rotational viscosity

Using linear response theory, Sarman and Evans [30] have shown that γ_1 can be derived from the integral of director angular velocity correlation function by

$$\gamma_1 = \frac{k_B T}{V \int_0^\infty dt \langle \Omega_2(t) \Omega_2(0) \rangle} \quad (2)$$

where T is the temperature, V is the volume and k_B is the Boltzmann's constant. However, an equivalent expression involving the mean squared displacement of director which has more definite physical meaning has been used:

$$\gamma_1 = \lim_{t\to\infty} \lim_{V\to\infty} \frac{2k_B T t}{V \langle |\vec{n}(t) - \vec{n}(0)|^2 \rangle} \quad (3)$$

Here, $\langle |\vec{n}(t) - \vec{n}(0)|^2 \rangle$ is called the director mean-squared displacement (DMSD), $\vec{n}$ is the director of LCs, which is often obtained from the second rank ordering tensor:

$$Q_{\alpha\beta} = \frac{1}{N} \sum_{j=1}^{N} \frac{3}{2} a_{j\alpha} a_{j\beta} - \frac{1}{2} \delta_{\alpha\beta} \quad (4)$$

where N is the number of molecules, α_j represents the long axis direction of each molecule which is found by diagonalising the inertia tensor. Usually, the nematic director is the eigenvector associated with the largest eigenvalue (order parameter S) of $Q_{\alpha\beta}$. At long times, the DMSD takes on a linear form and then, γ_1 can be calculated from the gradient of DMSD. What's more, averaging over many time origins and many times has been tried for good statistics.

2.3. Simulation details

The well-known simulated annealing was implemented in order to obtain various metastable states and observe the phase-transition temperatures between them. Then, long equilibration runs were performed for various LCs starting from the state after annealing, the director and order parameter were monitored throughout the simulations, the DMSD and γ_1 were finally achieved by averaging over many time origins, and of course, averaging over several sampling times is required for good statistics.

Specifically, MD simulations were initially carried out on an idealised cubic lattice of 200 molecules orientated with almost random order at a gas phase density. Each system was compressed rapidly by using a Berendsen isothermal–isobaric algorithm with a nominal pressure of 10^4 bar to reach the real density (about 1 g cm^{-3}). Thereafter, a 10-ns run was performed to equilibrate the system at a pressure of 1 bar and temperature of 800 K, which serves as a starting point to cool. The annealing protocol was specified as a series of corresponding reference temperatures and times. We were able to approximately predict the phase-transition temperatures by monitoring the director and order parameter in the process. Further runs (25 ns) were carried out at a series of temperatures to confirm the phase-transition temperatures and calculate the DMSD and γ_1 by recording the stability of order parameter of each system. Electrostatic interactions were calculated using a Particle-mesh Ewald (PME) summation with a cutoff of 10 Å. Also, the short ranged van der Waals interactions were truncated using a cutoff of 10 Å. All calculations were performed in the NPT ensemble using a v-rescale thermostat and a Berendsen barostat. In addition, all the simulations were run using a time-step of 1 fs and no bond constraint was used. The MD simulations were performed using the Gromacs package [31–33], version 5.1.1, on four processors with GPU acceleration.

3. Results and discussion

3.1. Phase state

Three different kinds of fast response LCs which are indicated as PPP(3,5F)3NCS, PPTP(3F)2NCS and PPTP(3,5F)3NCS [34], respectively, are shown in Figure 1. The former LC has a terphenyl unit in the rigid core while the latter ones have phenyl–tolane structures. The other similar structures extend the π-electron conjugation while retaining a suitable phase-transition temperature and a relatively low rotational viscosity.

The phases after annealing from 800 to 300 K are presented in Figure 2. We note that all LCs exhibit a disordered state at a high temperature section (about 800 K) which is called isotropic phase, and then, an

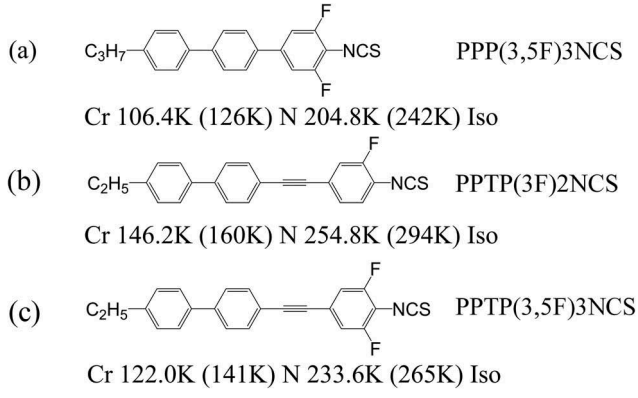

Figure 1. The molecular structures of fast response LCs which are indicated as (a) PPP(3,5F)3NCS, (b) PPTP(3F)2NCS and (c) PPTP(3,5F)3NCS.

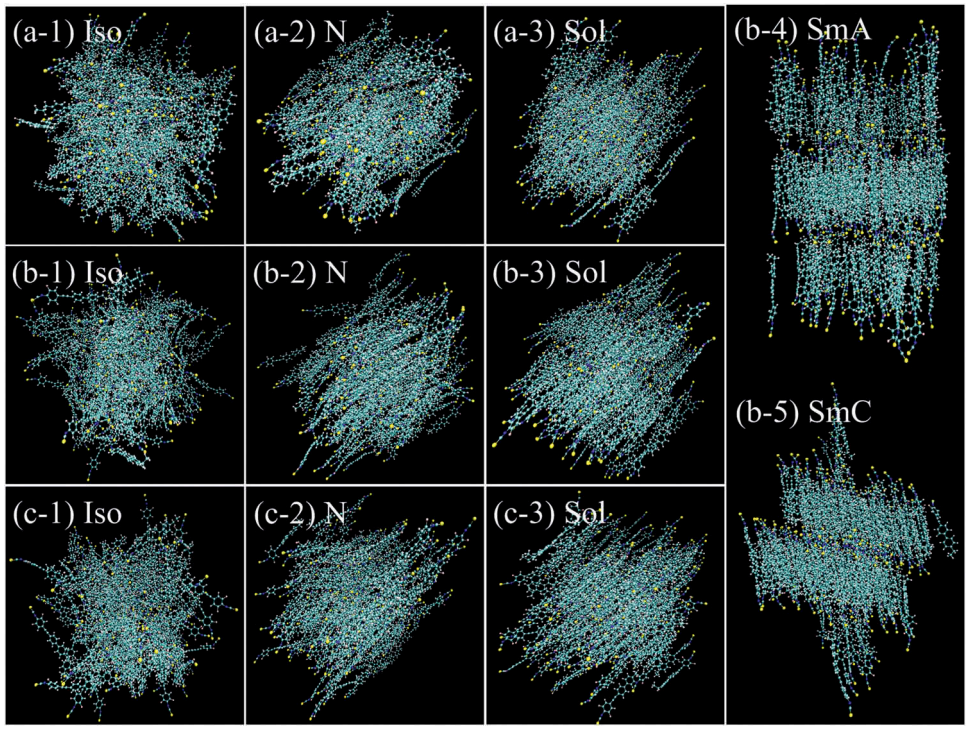

Figure 2. Various phase states of three different kinds of fast response LCs: (a-1) PPP(3,5F)3NCS, a liquid state; (a-2) PPP(3,5F)3NCS, a nematic state; (a-3) PPP(3,5F)3NCS, a solid state; (b-1) PPTP(3F)2NCS, a liquid state; (b-2) PPTP(3F)2NCS, a nematic state; (b-3) PPTP (3F)2NCS, a solid state; (b-4) PPTP(3F)2NCS, a smectic (SmA) state; (b-5) PPTP(3F)2NCS, a smectic (SmC) state; (c-1) PPTP(3,5F)3NCS, a liquid state; (c-2) PPTP(3,5F)3NCS, a nematic state; (c-3) PPTP(3,5F)3NCS, a solid state.

orientationally ordered state called nematic phase appears at a given time. With further decreasing of temperature, a smectic phase may be observed, like PPTP(3F)2NCS (Figure 2, b-4 and b-5), which is characterized by the layering normal or tilted to the director. So, it can be said that we are able to show the growth of a nematic phase or a smectic phase directly from an isotropic liquid over a 100-ns period for an all-atom model. However, according to experimental data [34], the smectic phase is not observed in all LCs, which suggests that the interaction between molecules may be very slightly too high in our model.

In order to obtain the phase-transition temperatures, the instantaneous LC order parameter was recorded during the growth of a liquid state, a nematic state and a solid (or smectic) state from an isotropic starting point (as illustrated in Figure 3). It can be clearly seen that the order parameter has a large fluctuation within a wide temperature region from 800 to 600 K and it is almost equal to zero. With further decreasing of temperature, the order parameter increases suddenly at a given time, which is a typical trait of nematic phase. Therefore, we can deduce that the N–I phase-transition temperature is 242, 294 and 265 K for PPP (3,5F)3NCS, PPTP(3F)2NCS and PPTP(3,5F)3NCS, respectively (as shown in Table 1). At around 150 K, we start to see some evidence for solidification/crystal

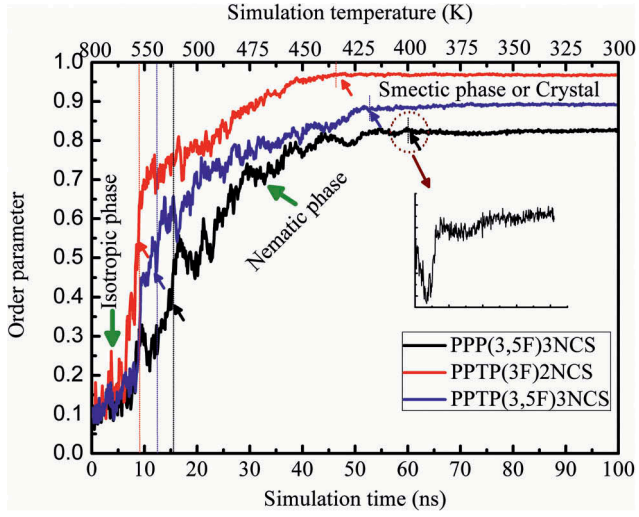

Figure 3. Time (or temperature) evolution of the instantaneous order parameter during the growth of a liquid state, a nematic state and a solid (or smectic) state from an isotropic starting point.

formation, with an accompanied lowering in fluctuation of orientational order but this process occurs relatively slowly. Of course, at this time, the order parameter keeps a constant value from macroscopic aspects. Consequently, our prediction for Sol-N (or Sm-N) transition temperature

Table 1. The phase-transition temperatures, birefringence Δn, rotational viscosity γ_1 and FoM of PPP(3,5F)3NCS, PPTP(3F)2NCS and PPTP(3,5F)3NCS.

LC	T_{mp} (°C)	T_c (°C)	Δn	γ_1(mPa s)	FoM ($\mu m^2 s^{-1}$ K_{11} = 30 pN)
			T (°C) = 50/100/150/200/250	50/100/150/200/250	50/100/150/200/250
PPP(3,5F)3NCS	126(19.6)	242(37.2)	0.44/0.43/0.40/0.31/0.08	186/169/129/117/103	31.2/32.8/37.2/24.6/1.9
PPTP(3F)2NCS	160(13.8)	294(39.2)	0.50/0.50/0.49/0.40/0.33	156/130/106/87/66	48.1/57.7/68.0/55.2/49.5
PPTP(3,5F)3NCS	141(19.0)	265(31.4)	–	–	–

is 126, 160 and 141 K, respectively (as shown in Table 1). In fact, once a LC phase had been obtained, more runs were carried out at a series of temperatures for further verification of phase-transition temperature. The instantaneous LC order parameter of PPP(3,5F)3NCS at different simulation temperatures has been given in Figure 4. The fluctuations of order parameter at different simulation temperatures are similar to those depicted in Figure 3. Especially, the blue line represents a state close to the clearing temperature (242 K) which is characterised as a partially ordered state with a large fluctuation of the instantaneous LC order parameter. We note that both clearing point and melting point are higher than the values reported by Gauza etc. [34] and the deviations are a little different. But despite all that, the simulations here correctly predict the phase-transition temperatures once those deviations can be taken into consideration. In other words, we can sort the fast response LCs by the calculated clearing point or melting point, which is very helpful in designing a low phase-transition temperature LC with high birefringence Δn simultaneously.

3.2. Rotational viscosity and response performance

Shown in Figure 5 are the DMSDs of PPP(3,5F)3NCS (solid lines) and PPTP(3F)2NCS (dotted lines) at different temperatures. In fact, each statistic was gathered over a 25-ns production run. In order to remove the effect of origin of statistic, the DMSDs were achieved by averaging over many time origins (about 10,000) with a 10-ns production run. In addition, a better statistics had been obtained by averaging over several sampling times. As can be seen, after an initial rapid rise, the DMSD takes on a linear form at long times. The calculated values of γ_1 at different temperatures are listed in Table 1. Obviously, with the temperature increasing from 50 to 250°C, γ_1 of both LCs decreases gradually. What's more, the γ_1 of PPP(3,5F)3NCS is significantly higher than that of PPTP(3F)2NCS, which may be caused by the following several aspects: Firstly, the terphenyl of PPP(3,5F)3NCS is more flexible than the phenyl-tolane of PPTP(3F)2NCS which serves as a rigid core. Furthermore, the difluoro substituent of PPP(3,5F)3NCS has a higher polarisability which confers greater intermolecular dispersion interactions. Finally, often, members with shorter alkyl chain have a lower rotational viscosity than those with a longer alkyl chain.

We calculated the birefringence Δn of nematic LCs (Table 1) by using the Vuks equation, among which the polarisability was obtained using the AM1 method which has been proved to be useful for predicting the birefringence [25]. In particular, the change of birefringence results from decreasing of order parameter with temperature increasing. According to the results above,

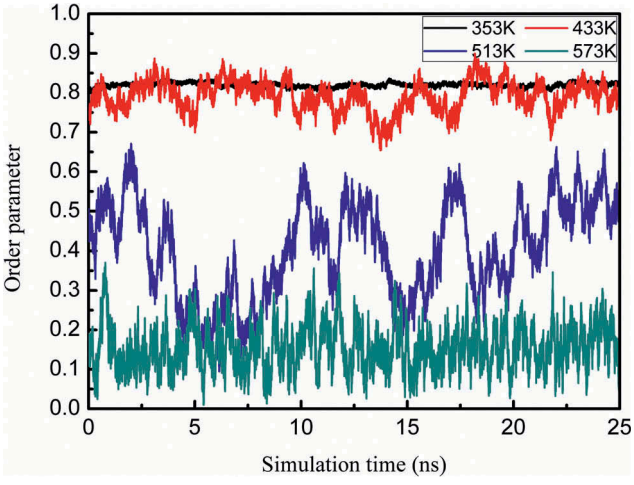

Figure 4. Time evolution of the instantaneous LC (PPP(3,5F)3NCS) order parameter at different simulation temperatures.

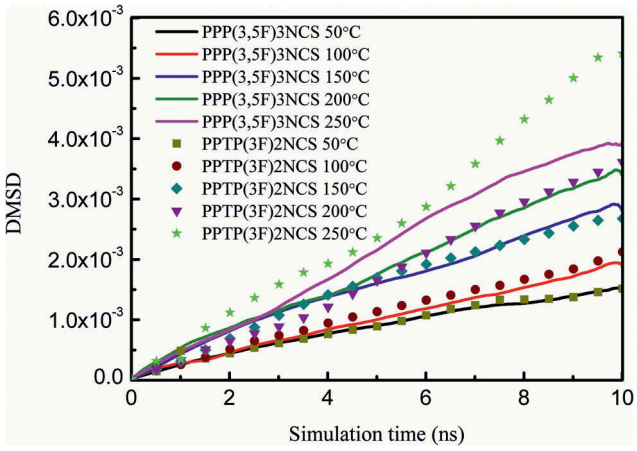

Figure 5. The director mean squared displacement (DMSD) of PPP(3,5F)3NCS (solid lines) and PPTP(3F)2NCS (dotted lines) at different temperatures shown as a function of time.

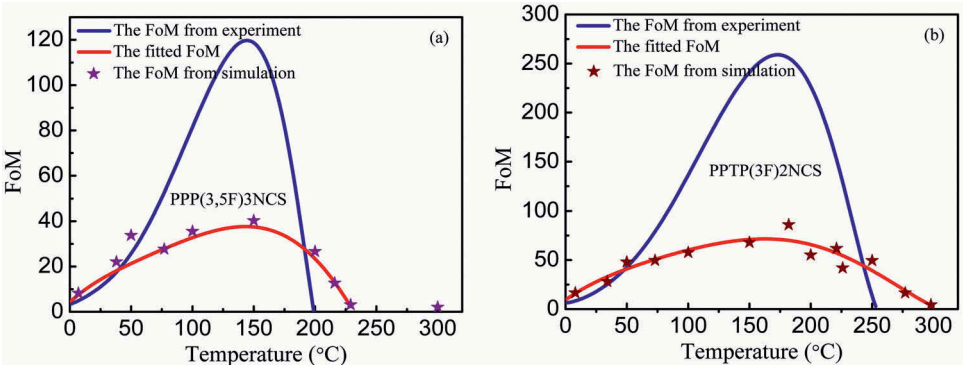

Figure 6. The temperature dependent FoM of (a) PPP(3,5F)3NCS and (b) PPTP(3F)2NCS. The blue lines are experimental results and the red lines or asterisks are calculated results.

the temperature dependent FoM of PPP(3,5F)3NCS and PPTP(3F)2NCS had been obtained (the K_{11} is taken as constant). As shown in Figure 6, the calculated FoM increases as the operating temperature increases and then decreases rapidly as the temperature approaches the clearing point, which is consistent with experiment results. In other words, they can both be fitted by the following equation [25]:

$$\mathrm{FoM} \propto \Delta n_{\mathrm{o}}^2 \left(1 - \frac{T}{T_{\mathrm{c}}}\right)^{3\beta} \exp\left(-\frac{E}{kT}\right) \tag{5}$$

where Δn_o is the birefringence in completely ordered state ($S = 1$), T_c is the clearing temperature. E is activation energy of the LC and k is the Boltzmann constant. The value of the β parameter is around 0.25 and insensitive to LC structures. Although there are some differences between the absolute values of FoM, the relative values of calculated FoM agree well with the experimental results. For example, their FoM at $T \sim 150$°C experimentally reaches 250 and 120 μm^2/s, respectively, and the ratio is about 2. Correspondingly, the calculated FoM at $T \sim 150$°C is 68.0 and 37.2 μm^2/s, respectively; so, the ratio is about 1.8 which is close to the experimental one. We deduce that the reason for the deviations of absolute values of FoMs is the overestimation of attraction between and within molecules. Specifically, both the flexible aromatic groups and alkyl chains between and within molecules which are slightly too attractive in the GAFF lead to a density that is slightly too high, resulting in over stabilisation of LC phases. Therefore, the phase-transition temperatures were overestimated by 20–40 K. What's more, the overestimation of the attraction in the GAFF further leads to a systematic shift in rotational viscosities. As mentioned above, the birefringence Δn of nematic LCs can be well predicted by using the Vuks model. Ultimately, the overestimation of rotational viscosities mainly leads to a systematic reduction of FoMs for fast response LCs.

4. Conclusions

In summary, in this paper, we have carried out all-atom MD simulations to evaluate the phase state and rotational viscosity of fast response LCs. The phase-transition temperatures between metastable states, rotational viscosity and response performance of such LCs have been successfully predicted. This work presented here opens up the possibility of using fully atomistic simulation as a means of rationally designing a fast response LC compound.

Significant overestimation of the attraction both between and within molecules in our model was observed. As a result, there are some deviations between the theoretical results and actual values. The next step in our work is towards further amendment to the intermolecular potential used in our model. Of course, system size effect and simulation procedure will also be further optimised. This work is underway in our laboratory.

Acknowledgements

This work was supported by the National Science Foundation of China (11604327, 61378075, 61377032, 61475152 and 61405194) and State Key Laboratory of Applied Optics, Changchun Institute of Optics, Fine Mechanics and Physics, Chinese Academy of Sciences.

Disclosure statement

No potential conflict of interest was reported by the authors.

Funding

This work was supported by the National Science Foundation of China: [11604327, 61378075, 61377032, 61475152 and 61405194] and State Key Laboratory of Applied Optics, Changchun Institute of Optics, Fine Mechanics and Physics, Chinese Academy of Sciences.

References

[1] Song H, Fraanje R, Schitter G, et al. Controller design for a high-sampling-rate closed-loop adaptive optics system with piezo-driven deformable mirror. Eur J Control. 2011;17:290–301.

[2] Beckers JM. Adaptive optics for astronomy-principles, performance, and applications. Annu Rev Astron Astrophys. 1993;31:13–62.

[3] Zhang Z, You Z, Chu D. Fundamentals of phase-only liquid crystal on silicon (LCOS) devices. Light Sci-Appl. 2014;3:e213.

[4] Hu HB, Hu LF, Peng ZH, et al. Advanced single-frame overdriving for liquid-crystal spatial light modulators. Opt Lett. 2012;37:3324–3326.

[5] Wu ST, Wu CS. Small-angle relaxation of highly deformed nematic liquid-crystals. Appl Phys Lett. 1988;53:1794–1796.

[6] Wang QD, Peng ZH, Yao LS, et al. The optimal cell gap determination of a liquid crystal wavefront corrector from a single photoelectric measurement. Liq Cryst. 2014;41:1569–1574.

[7] Restaino SR, Dayton D, Browne S, et al. On the use of dual frequency nematic material for adaptive optics systems: first results of a closed-loop experiment. Opt Express. 2000;6:2–6.

[8] Burns DC, Underwood I, Gourlay J, et al. A 256x256 sram-xor pixel ferroelectric liquid-crystal over silicon spatial light-modulator. Opt Commun. 1995;119:623–632.

[9] Love GD, Kirby AK, Ramsey RA. Sub-millisecond, high stroke phase modulation using polymer network liquid crystals. Opt Express. 2010;18:7384–7389.

[10] Huang XM. Thresholdless of ferroelectric liquid crystals. Chin J Liq Cryst. 2001;16:81–90.

[11] Gauza S, Jiao M, Wu ST, et al. High birefringence and low viscosity negative dielectric anisotropy liquid crystals. Liq Cryst. 2008;35:1401–1408.

[12] Gauza S, Wen CH, Wu B, et al. High figure-of-merit nematic mixtures based on totally unsaturated isothiocyanate liquid crystals. Liq Cryst. 2006;33:705–710.

[13] Vuks MF. Determination of the optical anisotropy of aromatic molecules from the double refraction of crystals. Opt Spectrosc+. 1966;20:361–368.

[14] Wilson MR. Progress in computer simulations of liquid crystals. Int Rev Phys Chem. 2005;24:421–455.

[15] Pelaez J, Wilson M. Molecular orientational and dipolar correlation in the liquid crystal mixture E7: a molecular dynamics simulation study at a fully atomistic level. Phys Chem Chem Phys. 2007;9:2968–2975.

[16] Care CM, Cleaver DJ. Computer simulation of liquid crystals. Rep Prog Phys. 2005;68:2665–2700.

[17] Chami F, Wilson MR, Oganesyan VS. Molecular dynamics and EPR spectroscopic studies of 8CB liquid crystal. Soft Matter. 2012;8:6823–6833.

[18] Kuwajima S, Manabe A. Computing the rotational viscosity of nematic liquid crystals by an atomistic molecular dynamics simulation. Chem Phys Lett. 2000;332:105–109.

[19] Zakharov AV, Komolkin AV, Maliniak A. Rotational viscosity in a nematic liquid crystal: a theoretical treatment and molecular dynamics simulation. Phys Rev E. 1999;59:6802–6807.

[20] Cheung DL, Clark SJ, Wilson MR. Calculation of the rotational viscosity of a nematic liquid crystal. Chem Phys Lett. 2002;356:140–146.

[21] Ilk Capar M, Cebe E. Rotational viscosity in liquid crystals: A molecular dynamics study. Chem Phys Lett. 2005;407:454–459.

[22] Kim JS, Jamil M, Jung JE, et al. Rotational viscosity calculation method for liquid crystal mixture using molecular dynamics. J Inf Display. 2011;12:135–139.

[23] Kim J, Jamil M, Jung JE, et al. Investigating the calculation of rotational viscosity of the mixture comprising different kinds of liquid crystals: molecular dynamics computer simulation approach. Chinese J Chem. 2011;29:48–52.

[24] Cheung DL. Structures and properties of liquid crystals and related molecules from computer simulation. Durham: University of Durham; 2002.

[25] Sebastian G, Haiying W, Chien-Hui W, et al. High birefringence isothiocyanato tolane liquid crystals. Jpn J Appl Phys. 2003;42:3463.

[26] Wang J, Wolf RM, Caldwell JW, et al. Development and testing of a general amber force field. J Comput Chem. 2004;25:1157–1174.

[27] Özpınar GA, Peukert W, Clark T. An improved generalized AMBER force field (GAFF) for urea. J Mol Model. 2010;16:1427–1440.

[28] Duan Y, Wu C, Chowdhury S, et al. A point-charge force field for molecular mechanics simulations of proteins based on condensed-phase quantum mechanical calculations. J Comput Chem. 2003;24:1999–2012.

[29] Cornell WD, Cieplak P, Bayly CI, et al. Application of RESP charges to calculate conformational energies, hydrogen bond energies, and free energies of solvation. J Am Chem Soc. 1993;115:9620–9631.

[30] Sarman S, Evans DJ. Statistical mechanics of viscous flow in nematic fluids. J Chem Phys. 1993;99:9021–9036.

[31] Abraham MJ, Murtola T, Schulz R, et al. GROMACS: high performance molecular simulations through multi-level parallelism from laptops to supercomputers. SoftwareX. 2015;1–2:19–25.

[32] Berendsen HJC, Van Der Spoel D, van Drunen R. GROMACS: a message-passing parallel molecular dynamics implementation. Comput Phy Commun. 1995;91:43–56.

[33] Van Der Spoel D, Lindahl E, Hess B, et al. GROMACS: fast, flexible, and free. J Comput Chem. 2005;26:1701–1718.

[34] Gauza S, Wu S-T, Spadło A, et al. High performance room temperature nematic liquid crystals based on laterally fluorinated isothiocyanato-tolanes. J Disp Technol. 2006;2:247–253.